Journal of Electrical Engineering 5 (2017) 171-180
doi: 10.17265/2328-2223/2017.04.001

Thermal Nonlinearity of Functionalized Graphene Enhanced by Gold Nanorods

Thekrayat Al Abdulaal[1] and Gregory Salamo[1, 2]

1. Microelectronics and Photonics Program, Institute for Nanoscience and Engineering, University of Arkansas, Fayetteville, AR 72701, USA

2. Physics Department, University of Arkansas, Fayetteville, AR 72701, USA

Abstract: The nonlinearity of functionalized and nonfunctionlaized graphene as well as gold nanorods were investigated using the Z-scan system with an Ar^+ laser beam tuned at a wavelength of 514 nm in a CW (continuous wave) regime that was in resonance with AuNRs (gold nanorods). Z-scan experimental study indicated that functionalized graphene had a negative nonlinear refraction with self-defocusing performance. The result concluded that gold nanorods (average length was 36 ± 3 nm, and the average diameter was 12 ± 2 nm) enhance the thermal nonlinear properties of graphene oxide materials. Gold nanorods were proved to enhance the nonlinear absorption by 50%, and there was a large enhancement on the thermal nonlinear refraction and the thermo-optical coefficient (dn/dT). It was observed that the AuFG (functionalized graphene film with gold nanorods) presented a large thermal nonlinear refraction. The value of the nonlinear refraction (n_1') of FG and AuFG samples was shifted from -0.533 × 10^{-7} cm^2/W to -2.92 × 10^{-7} cm^2/W. There was a large enhancement in thermal refraction value that was about five factors larger than the nonlinear refraction of the host material (FG) and much larger (4 orders of magnitude) than that for AuNRs.

Key words: Functionalized graphene, gold nanorods, nonlinear absorption, refractive index, thermal nonlinearity.

1. Introduction

Thermal lensing is the most significant phenomena that is the result of a laser beam with high power propagating through an absorbing material. Many years ago the thermal lens effect, as well as its applications, was extensively considered [1]. As a CW (continuous wave) laser interacts with a material, the material absorbs a small part of the laser energy, resulting in a local heating around the material [2]. Due to the fact that the material refraction mainly depends on temperature, laser absorption eventually results in raising the nonuniformity on the material refractive index in the transmission channel [2]. This nonuniformity is a dependent on the temperature and density of the laser transmission, resulting in the beam deforming. This absorbed material could be described as a lens that possibly increases the divergence of the laser beam [2].

Removing the produced heat efficiently has been considered a serious challenge to improve the reliability, quality and the performance of modern photonic, optoelectronic, and electronic systems such as supercomputers and cellphones [3]. Both experimental and even theoretical studies have proved that hot spots at micrometer or nanometer scale, created in nanoscale electronics with high power density due to the nonuniformity of the heat dissipation and generation, might lead to reliability problems and performance degeneration [4]. The previous cooling solutions, including semiconductor and metal nanomaterials, are limited because the thermal conductivity is low. Graphene has emerged to be a promising material of nanoscale heat spreading due to its enormously high thermal conductivity (κ), ranging from 2,000 to 5,000 W/m·K, at room temperature [3] as well as remarkable electrical, mechanical and optical properties. The great capability of handling CW laser is

Corresponding author: Thekrayat Al Abdulaal, Ph.D., assistant researcher, research fields: graphene materials, nonlinear properties, Z-scan technique.

widening the graphene application in photonics devices [5].

The graphene development of various functionality, structure, and sheet size has unique attention for different uses, such as metal nanoparticlesand oxygen groups [6]. The investigation of graphene oxide has received much attention due to the unique physical and chemical properties and how they may be applied to modern technologies [5]. Principally, graphene oxide, a nonlinear material with sufficient loss in linear regime, has become critically significant to protect devices by controlling the transmission signals [5]. Particularly, the nonlinearity of graphene oxide has been extensively studied, including nonlinear refraction, optical limiting, and saturable absorption. It was found that thin films of GO (graphene oxide) on glass substrates show remarkable broadband nonlinear properties [7]. GO is a monosheet of carbon atoms with oxygen groups, and the flexibility, conductivity, and strength are its most distinctive properties [8]. As demonstrated in Fig. 1, the GO structure exhibits epoxy, hydroxyl groups typically at the sheets' basal planes, while carboxyl and carbonyl are mostly located at the edges of the defects or sheets [8]. Those oxygen groups bind covalently to the surface of graphene that comprises a hybridized mixture of sp^3 and sp^2 carbon atoms and emerges as graphene oxide materials in a wide range of applications including photothermal, biosensors, optics, electronics, and energy fields, due to its unique optical and electrical properties [9].

Furthermore, MNPs (metal nanoparticles) have the ability to enhance absorbed and scattered light under appropriate optical radiation. Therefore, MNPs become an ideal heat source for the nanoscale, slightly well-regulated through light inputs [9]. A few years ago, MNPs (metallic nanoparticles) were also intensively investigated in nanoscale devices to control temperature [10]. Metal nanoparticles lead to the creation of enhanced electromagnetic fields that strongly affect the linear and nonlinear properties of the host material [10]. The nonlinear refraction of the material could be very high due to the change of the temperature around and within nanoparticles. AuNRs (gold nanorods) clearly present convincing enhancements in nonlinear properties of graphene materials due to their distinctive optical properties, especially plasmonic resonance. Gold nanorods are great converters of light energy to heat due to the coupling between the large absorption cross-section and the low radiative and fast nonradiative decay rate [11]. Thus, AuNRs could potentially be applied in photothermal therapy, optical limiting, imaging and sensing, cooling systems, energy storage, and in photovoltaic and thermal devices using CW lasers [6].

The energy band diagram of the AuFG (functionalized graphene sample with gold nanorods) explains the nonlinear absorption, shown in Fig. 2. The

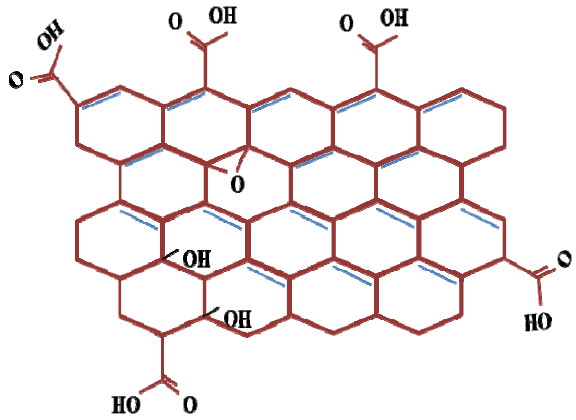

Fig. 1 Graphene oxide structure.

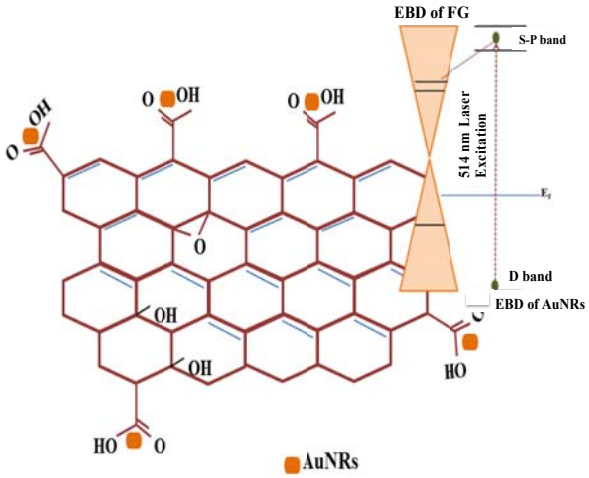

Fig. 2 EBD (energy band diagram) of the AuFG thin film sample under laser irradiation. Duplicated from Ref. [12].

FG material contains sp^3 matrix of oxygen group and sp^2 matrix of graphene while gold nanorods are generally attached to the FG sample through the oxygen containing groups [12]. This was using the first-principle calculation, where Subrahmanyam [12] illustrated that the metal intermediate energy states extend up to the GO conduction band in the nanocomposite case of metal-graphene. Free (d) electrons in gold move through the functionalized graphene material. The wavelength of the used laser is in resonance with the oscillations gold surface plasmon, which causes the free electrons in the gold nanorods to oscillate [12].

Experimentally speaking the thermal and optical nonlinear properties of AuFG (functionalized graphene with gold nanorods), then applying that in developing future optoelectronic devices, are still highly undeveloped. Because of the urgent needs in thermal management, optical limiting, and other thermal nonlinear devices, this research stems from this demand. Thus, the main objective of this research is to gain full understanding of the effects of the oxygen groups and gold nanorods on the thermal nonlinearity of graphene materials by using the Z-scan technique, which will help further a great revolution in nonlinear fields.

2. Experiments

The research investigated the nonlinear absorption coefficient (β) as well as nonlinear refraction (n_2) and thermo-optic coefficient (dn/dT), through building a simple, precise, and sensitive technique called Z-scan. Fig. 3 illustrates the experimental setup of the Z-scan measurements. The built Z-scan system uses a CW argon ion (Ar^+) laser at a wavelength of 514 nm in resonance with AuNRs plasmonic resonance peaks. The experimental procedure of building the Z-scan system is explained in detail in the main author's Ph.D. dissertation [1]. The Z-scan setup consists of an Ar^+ laser, a 5 cm focal length lens, a translation stage, a micrometer pinhole, and a silicon detector. In the Z-scan, the sample is fixed in a micrometer translation stage and is moved in the propagation direction (z) of a Gaussian beam that is narrowly focused. The transmitted signal is observed using a photo detector placed behind a small aperture as a function of the sample position relative to the beam waist.

The research samples were a collaborative work with Dr. Biris' group at the University of Arkansas in Little Rock. The samples under investigation were NFG (nonfunctionlaized graphene), FG (functionalized graphene), and AuFG (functionalized graphene with gold nanorods). All of the graphene-containing samples were thin films deposited on glass substrates, and as comparison gold nanorods (AuNRs) were studied alone diluted in a deionized water solution, as a reference sample. To summarize the preparation of these graphene films, first, single layer graphene flakes were purchased by Dr. Biris' group. Then, to embed AuNRs in the graphene, both were dispersed in a common solvent and filtered through a membrane. Finally, the graphene thin film was placed on a glass substrate by dissolving the membrane and washing the graphene film [13].

The unique physical morphology and structure properties of those graphene samples were investigated using different experimental optical and analytical techniques, including AFM (atomic force microscopy), and UV-VIS-NIR absorption spectroscopy. In addition, SEM (scanning electron microscopy) and TEM (transmission electron microscopy) were performed to

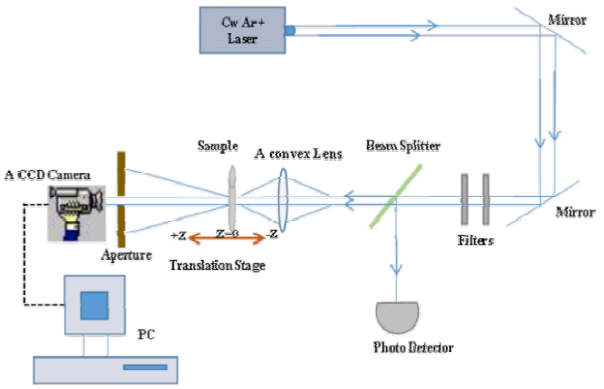

Fig. 3 Experimental setup of the Z-scan system.

determine the size, shape, and the concentration of gold nanorods in graphene films.

2.1 Structural Characterizations

Shimadzu Spectrophotometer (UV-3600) was used to linearly optically characterize graphene samples at room temperature. Experimentally, Fig. 4 illustrates the transmission spectra of the NFG, FG and AuFG films on glass substrates as well as the AuNRs sample in a deionized water solution in a 1 mm optical path quartz cuvette. Particularly at the light wavelength of 514 nm, the transmission of the FG sample was around 41.17%, while it was about 29.32% for the AuFG sample because of the gold nanorods.

It is shown that the FG film was more transparent than the NFG film because of oxygen groups in FG. Also, the transmittance spectra showed about 10% difference between the FG and AuFG; obviously, the AuNRs were the main cause of the difference. Here, the AuNRs transmission spectrum demonstrated two plasmonic resonance valleys at 514 nm and 730 nm, respectively (one because of the transverse electrons oscillation and two, due to the longitudinal electrons oscillation). Thus, there were little noticeable effects of the AuNRs plasmonic resonance on the AuFG thin film transmission spectra due to the AuNRs small concentration.

TEM was used to image gold nanorods, prepared through evaporating drops of the AuNRs solution on a carbon substrate, and to determine the length and width of gold nanorods by counting at least 50 nanorods, as illustrated in Fig. 5. These AuNRs are in an average diameter of 12 nm and length of 36 nm. The concentration of the gold nanorods on the functionalized graphene thin film sample was defined using the ESEM (environmental scanning electron microscopy) at low vacuum. TEM image was originally analyzed to be used in the calculation to determine the percentage of gold nanorods on the AuFG sample beside the ESEM image, shown in Fig. 6. TEM image shows a sufficient amount of gold nanorods

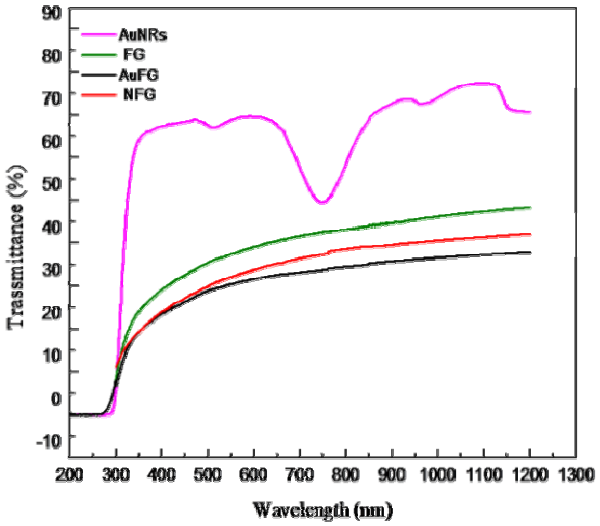

Fig. 4 Transmittance spectra of NFG, FG, AuFG and AuNRs materials.

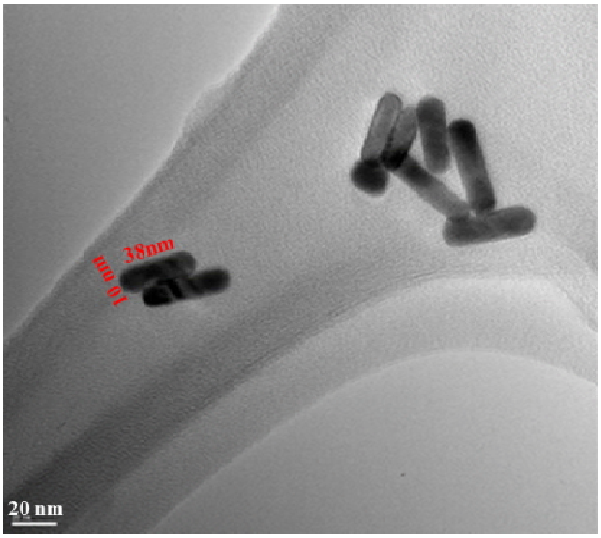

Fig. 5 TEM image of AuNRs on a carbon grid.

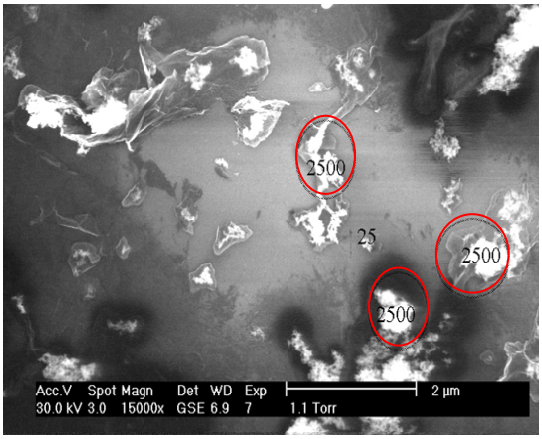

Fig. 6 ESEM image of the AuFG sample, bright area (in red circles) demonstrates AuNRs clusters.

was covering the FG (functionalized graphene) thin film sample. The concentration of AuNRs in the FG thin film sample was about 0.36% by weight.

The thickness of FG sample could be defined by the height difference along this cross-section line in the AFM image, as illustrated in Fig. 7. Also, the blue curve on the right of Fig. 8 is the average height in nanometers of the AuFG film. The average thickness of the AuFG film could be defined by the step height difference along this line. Thus, the AuFG average thickness was around 101 nm with ±50 nm of RMS roughness as an error bar. In the AFM image of the AuFG sample, as illustrated in Fig. 8, the gold nanorods appear like bright dots that slightly increased the film average thickness in comparison to the FG thickness. The average thickness of the FG sample was around 92 nm with ±45 nm of RMS roughness as an error bar. This suggests that the FG sample was not uniformly deposited on the glass substrate.

2.2 Nonlinear Measurements

The nonlinear absorption should be determined first since the closed aperture Z-scan data are sensitive to not only the nonlinear refraction but also to the nonlinear absorption. From the open aperture Z-scan measurements, the nonlinear absorption coefficient could be extracted. Then, from dividing the data of the closed aperture by the open aperture data of Z-scan measurements, the nonlinear refractive index could be determined. The nonlinear properties of NFG, FG, AuFG and AuNRs were measured using the Z-scan system, illustrated in Fig. 3.

2.3 Gold Nonlinear Results

After measuring the deionized water in a 1 mm quartz cell as background, the gold nanorods sample in a deionized water solution (AuNRs) was studied to determine the thermal nonlinear properties. Under the same conditions of Z-scan measurements, the deionized water did not show any nonlinear behaviors. Fig. 9 experimentally illustrates an example of an open aperture Z-scan configuration of AuNRs at various input laser power. Simply, the absorption depends linearly on the laser intensity, and the absorption coefficient could be written as [14]:

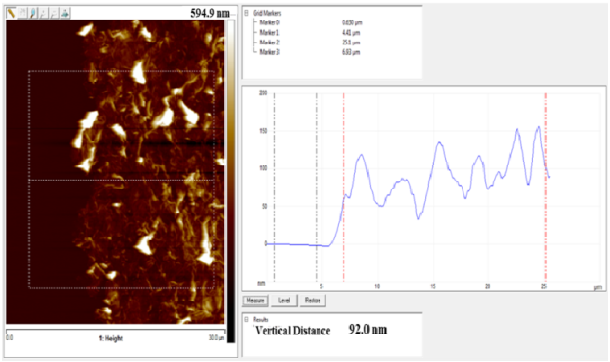

Fig. 7 AFM image of FG film with the thickness variation represented by the blue curve.

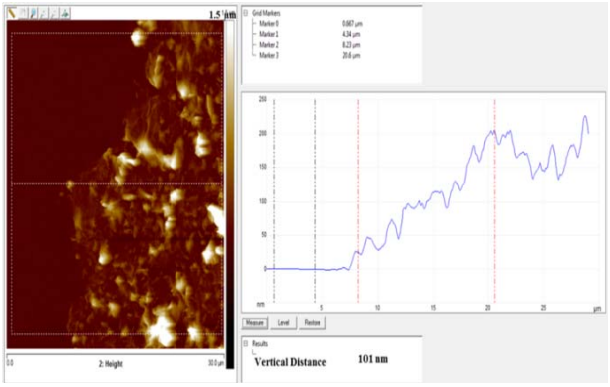

Fig. 8 Image of the AFM topography of AuFG.

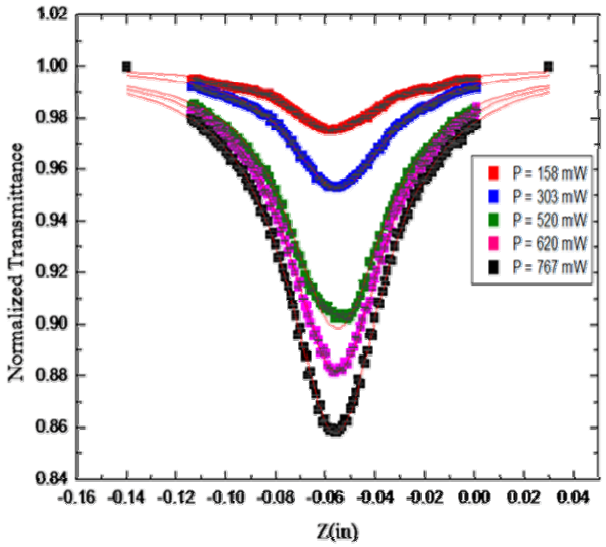

Fig. 9 Open aperture Z-scan data of AuNRs at different laser power; the red curves are the theoretical fitting.

$$\alpha(I) = \alpha_0 + \beta I \quad (1)$$

The data of NT (normalized transmittance) in Fig. 8 fit nicely with the theoretical model of the open aperture data of Z-scan measurements as given in Eq. (2).

$$NT\ (z, t) = -q_0\ [2.83\ (1+ (z/z_0)^2)]^{-1} + 1 \quad (2)$$

where, z is the material position, z_0 is the Rayleigh length ($z_0 = \pi\omega_0^2/\lambda$), ω_0 is the laser beam waist, λ is the laser wavelength, and the complex parameter (q_0) is linearly related to the nonlinear absorption (β) by:

$$q_0 = \beta\ I_0\ L_{eff},\ (|q_0| << 1) \quad (3)$$

where, I_0 is the laser intensity at the lens focus, and L_{eff} is the effective length of the sample ($L_{eff} = (1-e^{-\alpha L})/\alpha$), where L and α are the material thickness and linear absorption coefficient respectively. Here, β was a constant value that was considered as one of the material parameters.

Thus, the nonlinear absorption (β) of the AuNRs sample could be calculated by extracting the slope of β L_{eff} from Eq. (3), which clearly shows that β did not depend on the applied laser intensity. Thus, the value of the nonlinear absorption coefficient (β) for AuNRs was found to be approximately $0.215 \times 10^{-4} \pm 3.19E\text{-}6$ cm/W. These results indicated that there was heat accumulation inside the focal volume of the gold nanorods by absorption of CW Ar^+ laser, and the embedded AuNRs acted as absorbers of the CW laser energy in the nanoscale. Then, the laser energy transferred from the gold nanorods to their environment through phonon-phonon interactions, which caused the temperature of the focal volume to increase. As a result, the absorbed energy dissipated out from the focal volume to the bulk medium [11].

In the closed aperture measurements, a peak shadowed by a valley was shown in the normalized transmittance, as illustrated in Fig. 10. The unique shape of the closed aperture Z-scan data was a clear sign of a self-defocusing inside the AuNRs material. This self-defocusing behavior directed to a negative nonlinear refraction of the AuNRs sample. The thermal

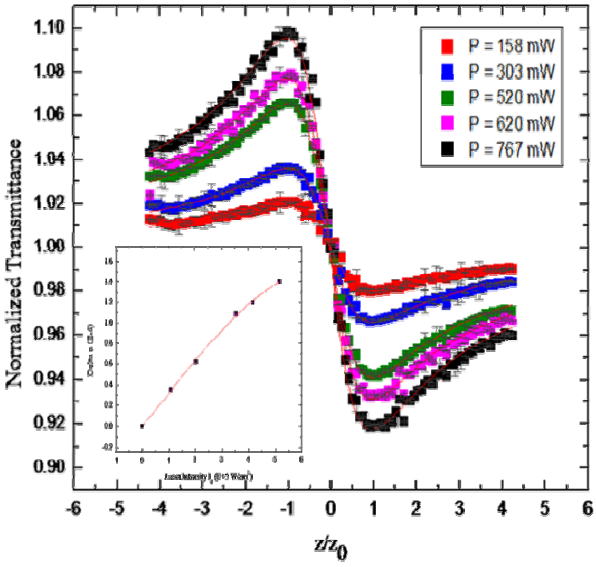

Fig. 10 Closed aperture Z-scan experimental results of the AuNRs sample at different laser power; the red curves are the theoretical fitting; insert is the refraction change (Δn) as a function of the laser intensity.

lens model was an excellent fit for the experimental data and was used to extract the phase shift at different laser powers. The theoretical equation to determine the change in the nonlinear refraction (n_1' and n_2') and thermo-optical coefficient (dn/dT) from the experimental data of Z-scan is expressed as [14]:

$$NT\ (z, t) = [1+ (\theta\ 2x/\ (1+ x^2))]^{-1} \quad (4)$$

where, NT (z, t) is the normalized transmittance a function of the sample position (z), $x=z/z_0$ is the normalized position, dn/dT is related to phase change (θ) by this relation:

$$\theta = \alpha PL/\lambda\kappa\ [dn/dT] \quad (5)$$

Eq. (6) defines the change in nonlinear refractive index (Δn) as:

$$\Delta n = [dn/dT]\ (I_0 \alpha w_0^2\ /4\kappa) \quad (6)$$

where, κ is the thermal conductivity and P is the laser input power. Thus, the magnitude of the obtained nonlinear refractive index (n_1') for the AuNRs material was calculated on the order of $-0.1 \times 10^{-9} \pm 1.65E\text{-}11$ cm^2/W. This value was based on the polynomial fitting of the refraction change versus the laser intensity, as illustrated in Fig. 10.

3. Z-Scan Measurements

3.1 Open Aperture

Both open aperture and closed aperture Z-scan measurements were applied to extract the nonlinear absorption and refraction coefficients, using the nonlinearity data of the glass substrate as a reference. The two-photon absorption of the FG, AuFG and NFG samples was studied using 514 nm with the Z-scan system, as illustrated in Fig. 11. This wavelength was roughly within the plasmon resonance peak. In open aperture measurements, the normalized transmittance was achieved as the film was transferred passing the lens focus. Once the sample moved closer to the focus, the beam intensity became higher, thus, the nonlinear absorption increased, which was leading to a decrease in the transmittance around the focus.

The value of nonlinear absorption (β) was calculated based on Eq. (3) after theoretically fitting all open experimental data using Eq. (2), and extracting the values of the complex parameter (q_0) at different input laser powers. For example, the value of the nonlinear absorption coefficient (β) for the AuFG film was derived from the linear fitting to the data in Fig. 12, and extracting the slope value. The nonlinear absorption coefficient (β) for the FG film was calculated to be 8.75 × 10^{-2} ± 0.0014 cm/W, whereas β value for AuFG was 12.8 × 10^{-2} ± 0.0015 cm/W at 514 nm wavelength. Moreover, the enhancement of the nonlinear absorption of the FG film compared to the NFG film (β = 1.58 × 10^{-2} ± 0.0016 cm/W), illustrated in Fig. 11, was because of the oxygen groups.

The open Z-scan experimental results show large enhancements in the nonlinear absorption of the AuFG film by 50% compared to that value for the FG film. It was a really huge enhancement where, for example, the β value of the AuFG sample was not the sum of β value for FG and β value for AuNRs. The β (AuFG) value was larger than β(FG) + β(AuNRs). As shown in Fig. 11, the AuFG had the largest valley among the open aperture curves of all the investigated samples, which took advantage of oxygen-containing groups as well as the plasmonic resonance of the gold nanorods. Thus, the AuFG film demonstrated much better nonlinear properties, as large as 8 times compared with the value for the NFG film. These open aperture Z-scan results indicated that the main cause of the thermal nonlinear absorption enhancement of the AuFG sample was the presence of the gold nanorods on the FG thin film sample.

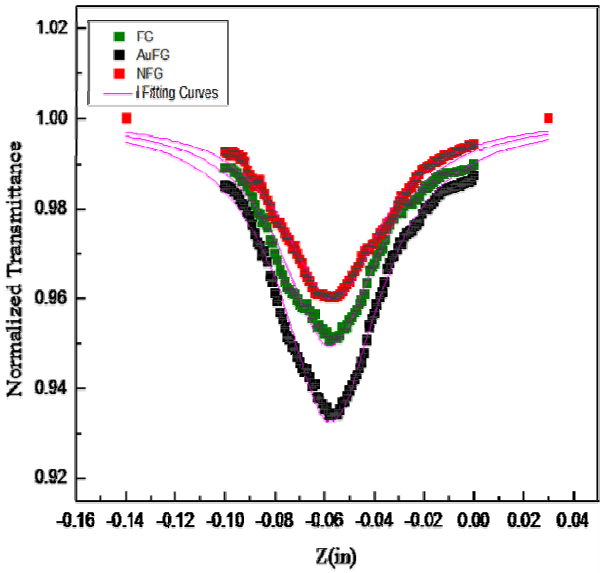

Fig. 11 Open aperture Z-scan of FG, AuFG and NFG samples at the same laser input power (303 mW).

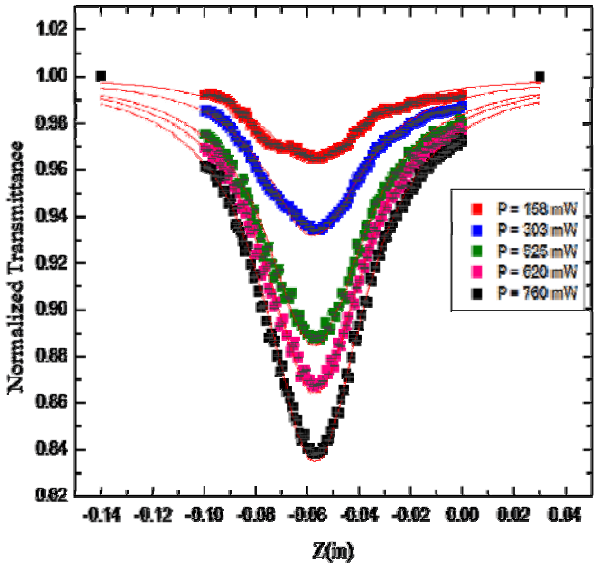

Fig. 12 Open aperture experimental data for the AuFG sample at different laser power.

3.2 Closed Aperture

The nonlinear absorption coefficient was measured first using the open aperture Z-scan measurements. Then from the closed aperture Z-scan, the nonlinear refractive index (n_1' and n_2') and the thermo-optic coefficient (dn/dT) were calculated. To evaluate the nonlinear refraction, closed aperture Z-scan measurements were accomplished for FG and AuFG thin films as a function of Ar^+ laser input power, respectively demonstrated in Figs. 13 and 14. Those closed aperture Z-scan data were divided by the data of open aperture scans and then the normalized transmittance data were plotted as a function of the sample normalized position ($x= z/z_0$). The closed aperture Z-scan experimental results were found to be in good agreement with the theoretical model of a thermal thin lens. The small error bars ensured the accuracy of the theoretical fitting curve to the experimental data. All Z-scan experimental curves demonstrated an asymmetric peak-valley pattern, which directly indicated a negative nonlinear refraction (n_1' and $n_2' < 0$), self-defocusing behavior.

Clearly, the value of the phase shift was raised with the increase of the Ar^+ laser power because of the rise in the temperature. It obviously suggested, from the observed linear dependences of ΔT_{p-v} on the laser powers, that thermal induced properties had a significant impact on the data of the Z-scan measurements. In the non-negligible case of the linear absorption, the temperature of the material was raised creating a thermal lens where the material refraction depended on the temperature ($dn/dT \neq 0$). As a consequence of the raised temperature, self-diffraction occurred, while dn/dT and n_1'&n_2', which were negative, were reduced. Therefore, this produced thermal lensing made a significant effect on the transmittance signal at the far field, in addition to the nonlinear response of the material. The effects of thermal lensing depended on the total heat transferred to the material, which is increased linearly with the laser power. The produced gradient of the refraction formed a thermal lens, a lens-like optical element, in Z-scan that resulted in the beam phase distortion at the far field of propagation.

The value of the phase shift, obtained from fitting Eq. (4), was linearly dependent on the laser power. The thermally induced phase shift (θ) and, thus, the thermo-optic coefficient (dn/dT) were not constant values, as illustrated in Eq. (5). Then, the change in the refractive index was found to apply the following expression in Eq. (6). Fig. 15 demonstrates the change

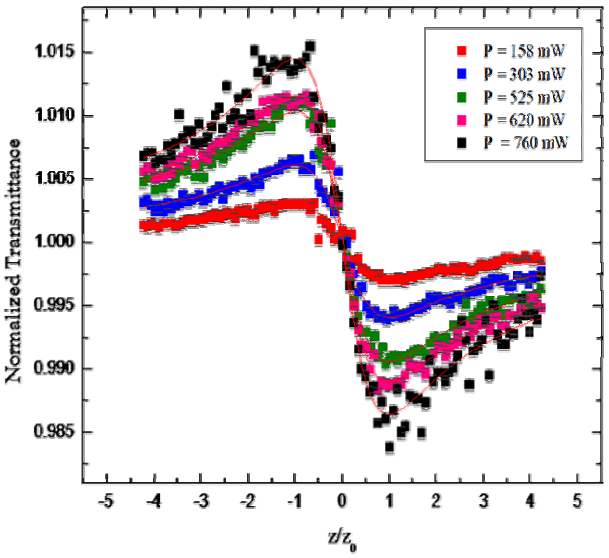

Fig. 13 Experimental closed aperture Z-scan results for the FG sample at different applied Ar^+ laser power.

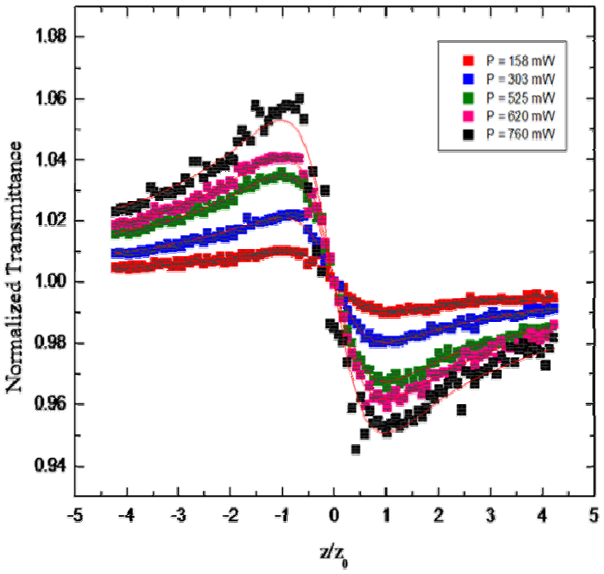

Fig. 14 Closed aperture data (normalized transmittance as a function of the AuFG position) at various laser power.

in the refractive index of the FG and AuFG samples versus the applied laser intensities, and those data were fitted with a second order polynomial equation to extract the nonlinear refraction value.

This fitting resulted in a value of -0.533 × 10^{-7} ± 0.017E-8 cm^2/W and -2.92 × 10^{-7} ± 0.0314E-8 cm^2/W for the nonlinear refractive index of the FG and AuFG films, respectively. The AuFG boosted the nonlinear refraction as much as five times that of the reference FG film. Moreover, gold nanorods gave significant enhancement in the n_2' value for AuFG that is much larger, around 13 times the value of the host material (the FG film). The practical asymmetric behavior of the closed aperture data, in addition to the fact that the laser was a continuous wave light source, implied that the source of nonlinear refraction was due to thermo-optic effects. The linear and nonlinear parameters of the NFG, FG, and AuFG samples, as well as AuNRs are given in Table 1.

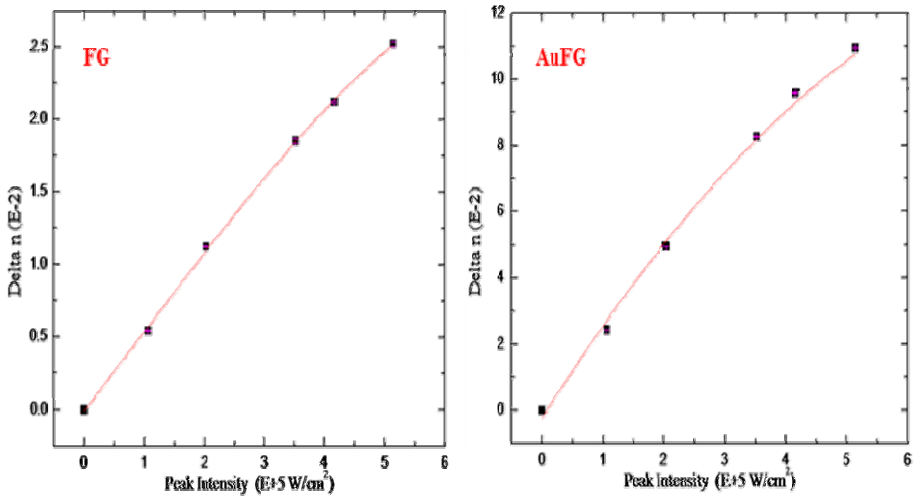

Fig. 15 Refraction change in the FG and AuFG samples versus laser intensity.

Table 1 Linear and nonlinear parameters of the NFG, FG, AuFG, and AuNRs samples at 514 nm wavelength.

Parameters	NFG	FG	AuFG	AuNRs
Linear Absorption (α) cm^{-1}	2.27 E+4	4.39 E+4	4.85 E+4	0.126 E+3
Linear Refractive Index (n_0)	2.141	1.85	2.36	2.314
Affective Thickness (L_{eff}) nm	254	92	101	36 x 12
Thermal Conductivity (κ) /K [37, 138]	1495	28.8	17.28	320
Thermo-optic Coefficient (dn/dT) /K	2.091 x 10^{-4} ± 2.63E-5	0.823 x10^{-6} ± 7.88 E-5	1.55 x 10^{-6} ± 1.402E-4	0.2301 x10^{-5} ± 8.33E-7
Nonlinear refractive Index (n_1`) cm^2/W	-1.5224 x 10^{-6} ± 2.37E-8	-0.533 x 10^{-7} ± 1.66 E-10	-2.92 x 10^{-7} ± 3.14E-10	-0.1 x 10^{-9} ± 1.65 E-11
Nonlinear refractive Index (n_2`) cm^4/W^2	-0.243 x 10^{-12} ± 0.0038 E-12	-0.0121 x 10^{-14} ± 0.0249 E-16	-0.154 x 10^{-14} ± 0.0591E-14	-0.042 x10^{-16} ± 0.023E-16
Nonlinear Absorption (β) cm/W	1.58 x 10^{-2} ± 1.67 E-3	8.75 x 10^{-2} ± 0.0014	12.8 x 10^{-2} ± 0.0015	2.15 x10^{-5} ± 3.19E-6
Change in Refractive Index (Δn)	0.0897	0.0012	0.0496	0.478x10^{-3}

4. Conclusions

In this work, the results of the experimental investigation of thermal nonlinearity of graphene based materials, including nonfunctionalized and functionalized graphene materials without and with gold nanorods (NFG, FG, and AuFG) have been presented. Z-scan technique was used to study the nonlinear properties using CW laser at 514 nm wavelength. These results highlight the important role of the gold nanorods and oxygen groups in the thermal nonlinearity of graphene materials. There was enormous enhancement in the thermo-optic coefficient of AuFG film owing to the presence of AuNRs and oxygen groups. The existence of groups on the surface of graphene materials enhances nonlinear properties while decreasing its essential electrical and thermal conductivity. Graphene and GO with gold nanorods is a great solution to manage thermal energy, thus, excellently spreading the generated heat in electronic devices because of its distinctive physical properties like large thermal conductivity and high transparency.

Acknowledgements

Thanks to Dr. Morgan Ware and Dr. Mourad Benamara for their help and significant discussions. A lot of thanks go to Dr. Biris's group at University of Arkansas in Little Rock on providing the research graphene samples.

References

[1] AlAbdulaal, T., Benamara, M., Ware, M., Saini, V., Biris, A., and Salamo, G. 2016. "Measuring Nonlinear Properties of Graphene Thin Films Using Z-Scan Technique." In *Proceedings of Physical Electronics PEC SM2001 Conference*, Fayetteville, Arkansas, USA.

[2] Mahdieh, M. H., and Jafarabadi, M. A. 2012. "Optical Characterization of Thermal Lens Effect in Ethanol and the Influence of Focusing Lens and Liquid Cell Size." *Optics & Laser Technology* 44 (1): 78-82.

[3] Nika, D. L., Yan, Z., and Balandin, A. A. 2015. "Thermal Properties of Graphene and Few-Layer Graphene: Applications in Electronics." *IET Circuits Devices Syst.* 9 (1): 4-12.

[4] Turin, V. O., and Balandin, A. A. 2006. "Electrothermal Simulation of the Self-heating Effects in GaN-based Field-Effect Transistors." *J. Appl. Phys.* 100 (5): 54501.

[5] Fraser, S., Zheng, X., Qiu, L., Li, D., and Jia, B. 2015. "Enhanced Optical Nonlinearities of Hybrid Graphene Oxide Films Functionalized with Gold Nanoparticles." *Appl. Phys. Lett.* 107 (3): 31112.

[6] Pezzi, L., De Sio, L., Veltri, A., Placido, T., Palermo, G., Comparelli, R., and Umeton, C. 2015. "Photo-Thermal Effects in Gold Nanoparticles Dispersed in Thermotropicnematic Liquid Crystals." *Physical Chemstry Chemical Physics* 17 (31): 20281-7.

[7] Hu, Y., and Su, X. 2013. "Chemically Functionalized Graphene and Their Applications in Electrochemical Energy Conversion and Storage." In *Advances in Graphene Science*, edited by Aliofkhazraei, M. InTech.

[8] Liu, Z., Zhang, X., Yan, X., Chen, Y., and Tian, J. 2012. "Nonlinear Optical Properties of Graphene-based Materials." *Chin. Sci. Bull.* 57 (23): 2971-82.

[9] Kravets, V. G., Marshall, O. P., Nair, R. R., Thackray B., Zhkov, A., Leng, J., and Grigorenko, A. N. 2015. "Engineering Optical Properties of a Graphene Oxide Metamaterial Assembled in Microfluidic Channels." *Opt. Express* 23 (2): 1265.

[10] Bigot, J.-Y., Halté, V., Merle, J.-C., and Daunois, A. 2000. "Electron Dynamics in Metallic Nanoparticles." *Chem. Phys.* 251 (1): 181-203.

[11] Yeup, G., and Hoon, C. 2009. "Simple Optical Methods for Measuring Optical Nonlinearities and Rotational Viscosity in Nematic Liquid Crystals." In *New Developments in Liquid Crystals*, edited by Kim, G. Y., and Kwak, C. H. InTech, 111-26.

[12] Biswas, S., Kole, A. K., Tiwary, C. S., and Kumbhakar, P. 2016. "Enhanced Nonlinear Optical Properties of Graphene Oxide-silver Nanocomposites Measured by Z-Scan Technique." *RSC Adv* 6 (13): 10319-25.

[13] Nima, Z. A., Lahiani, M. H., Watanabe, F., Xu, Y., Khodakovskaya, M. V., and Biris, A. S. 2014. "Plasmonically Active Nanorods for Delivery of Bio-Active Agents and High-Sensitivity SERS Detection in Planta." *RSC Adv* 4 (110): 64985-93.

[14] Kelley, P. L. 1965. "Self-focusing of Optical Beams." *Phys. Rev. Lett.* 15 (26): 1005-8.